Rayleigh Noise Reduction in 10-Gb/s Carrier-Distributed WDM-PONs Using In-Band Optical Filtering

Jing Xu, Ming Li, and Lian-Kuan Chen, *Senior Member, IEEE*

***Abstract*—To circumvent the challenging issue of Rayleigh noise reduction in wavelength-division-multiplexed passive optical network (WDM-PON), we provide an insight into the source of Rayleigh noise, and confirm that the suppression of carrier Rayleigh backscattering (RB) should be the primary target in the design of Rayleigh noise-resilient upstream receiver module for a transmission reach up to 60 km. Then we propose and demonstrate a novel scheme to effectively suppress the carrier RB in carrier-distributed WDM-PONs. By simply replacing the upstream modulation format of conventional on-off keying (OOK) with differential phase-shift keying (DPSK), the system tolerance to carrier RB is substantially enhanced by 19 dB, as the carrier RB can be considerably rejected by the notch filter-like destructive port of the delay-interferometer (DI) at the optical line terminal (OLT), which is used simultaneously to demodulate the upstream DPSK signal. The dependence of carrier RB suppression on DI's extinction ratio (ER) and optical carrier's line width is also theoretically analyzed. Experimental demonstration of 10-Gb/s upstream signal is achieved with less than 2.5-dB power penalty induced by Rayleigh noise after the transmission in 60-km single mode fiber, without using any amplifier in outside plant. The relation between system margin and the gain of optical network unit (ONU) is also studied.**

***Index Terms*—differential phase-shift keying (DPSK), optical access network, Rayleigh backscattering (RB), wavelength-division-multiplexed passive optical network (WDM-PON).**

I. Introduction

FORESEEING the rapidly growing demand for multimedia services and the trend of service convergence, the wavelength-division-multiplexed passive optical network (WDM-PON) is a promising technology to provide next-generation broadband access that requires large dedicated symmetric bandwidth and upgrade flexibility [1]. The colorless optical network unit (ONU) is essential for low-cost implementation of WDM-PON, as it can move the function of wavelength provisioning, monitoring and stabilization from individual ONUs to the common central office. Furthermore, colorless ONUs can greatly facilitate mass production and the operation, administration, and maintenance (OA&M) functions, as identical modules are used by all ONUs. Centralized carrier distribution is a promising approach to realize broadband (10 Gbit/s or above) colorless ONU, in which the upstream optical carriers are remotely distributed from the optical line terminal (OLT) to each ONU [2], [3]. In the carrier-distributed architecture, however, the upstream signal is susceptible to the interferometric crosstalk induced by the beating between the upstream signal and the Rayleigh backscattering (RB) of the distributed optical carrier, both of which are of the same wavelength [4]. Intensive studies have been carried out to mitigate this interferometric crosstalk. They are well summarized in [5] and [6]. Reducing the light source coherence is the most straightforward approach to reduce the impact of interference [7], [8]. However, this scheme is vulnerable to dispersion. After detection the beating noise mainly distributes at the low frequency region, and thus can be suppressed by an electrical high-pass filter (HPF) [9]–[11]. These schemes require only minor modifications to the PON structure. However, proper line coding [9], [10], or electrical equalization [11], is needed to alleviate the HPF-induced distortion to the upstream signal. In addition, the reported improvement in Rayleigh noise tolerance is limited to 5 dB [9], [11]. Although in [10] the improvement in Rayleigh noise tolerance can be more than 10 dB, the signal extinction ratio (ER) has to be lower than 6 dB. Besides these electrical-domain approaches, the Rayleigh noise can also be circumvented directly in optical domain, which turns out to be more effective [12]–[17]. The carrier RB light towards the OLT, with a narrow spectrum, can be effectively suppressed by an optical notch filter. However, Rayleigh noise is an in-band noise with heavy spectral overlap with the upstream signal, imposing significant challenges in directly filtering out the Rayleigh noise without impairing the upstream signal itself. Thus, to mitigate the impairment to the upstream signal induced by the optical notch filter, several approaches have been proposed to spectrally up-shift the upstream signal, using additional phase modulation [12]–[14], sub-carrier multiplexing (SCM) [15], or carrier suppressed subcarrier amplitude modulated phase modulation [16]. Although reported as very effective (the improvement in Rayleigh noise tolerance can be 17 dB [16]), these approaches are constrained by poor dispersion tolerance [12]–[15], requiring additional external modulators at ONU [13], [14], and complicated de/modulation circuits [16]. These constraints actually originate from the spectral up-shifting of the upstream signal.

Recently, we proposed a simple scheme, via in-band optical filtering, to reduce RB in the carrier-distributed WDM-PON

Manuscript received May 30, 2011; revised September 25, 2011, October 21, 2011; accepted October 21, 2011. Date of publication October 28, 2011; date of current version December 02, 2011. This work was supported in part by research grants from Hong Kong Research Grants Council (Project No: 410908).

The authors are with the Department of Information Engineering, The Chinese University of Hong Kong, Shatin, N. T., Hong Kong SAR, China (e-mail: xj007@ie.cuhk.edu.hk; mingli@ie.cuhk.edu.hk; lkchen@ie.cuhk.edu.hk).

Color versions of one or more of the figures in this paper are available online at http://ieeexplore.ieee.org.

Digital Object Identifier 10.1109/JLT.2011.2173904

[18]. By replacing the conventional on-off keying (OOK) modulation format in upstream with differential phase-shift keying (DPSK), the upstream signal is able to pass through an optical notch filter, which is used to reduce the RB light, without any impairment. At any rate an optical notch filter, such as the destructive port of a delay-interferometer (DI), is required to demodulate the upstream DPSK signal. As no deliberate spectral up-shifting is required in this scheme, neither additional modulator nor complicated modulation/demodulation circuit is needed at ONU/OLT. In terms of the optical notch filter used to reduce the RB light, the standard DI used in the proposed scheme is also more favorable than the non-standard filters that are either specially designed ultra-narrow notch filters or wavelength-detuned arrayed waveguide gratings (AWG) used in the prior schemes [13], [14], [16]. In this paper, we further investigate different issues for the Rayleigh noise reduction in carrier-distributed WDM-PON, with emphasis on building a comprehensive theoretical model to guide system design. It is widely reported that both types of RB (the carrier RB and the signal RB) induce crosstalk to the upstream signal [14], [16], [19], [20]. Increasing the ONU gain will increase the signal-to-carrier RB ratio, but will decrease the signal-to-signal RB ratio [19]. For this reason, both types of RB need to be considered in optimizing ONU gain if no measure is taken to suppress the Rayleigh noise entering upstream receivers. In this paper, we characterize the different weights of two types of RB in a WDM-PON with Rayleigh noise-reduced upstream receivers. It is found that the carrier RB is dominant within a reach up to 60 km; thus effective suppression of carrier RB is essential in the design of Rayleigh noise-immune upstream receivers. We then experimentally demonstrate that the proposed scheme can substantially improve the system tolerance to carrier RB by 19 dB. We also theoretically study the dependence of carrier RB suppression on DI's ER and optical carrier's line width. Experimental demonstration of 10-Gb/s upstream signal over 60-km standard single mode fiber (SMF) is achieved with less than 2.5-dB power penalty induced by Rayleigh noise, thanks to the effective suppression of the dominant carrier RB. We also investigate the relation between system margin and ONU gain, based on which the maximum system reach can be predicted.

The paper is organized as follows. In Section II, we discuss the proposed system architecture and analyze the different roles played by two types of RB in impairing the upstream signal. Section III reports the effectiveness of the proposed scheme on RB reduction, followed by a transmission demonstration. The dependence of the proposed scheme on DI's ER and optical carrier's line width is also theoretically studied. The relation between system margin and ONU gain is investigated in Section IV. Finally, conclusion is given in Section V.

II. Proposed System Architecture and the Source of Rayleigh Noise

A. System Architecture

Fig. 1 shows the proposed loopback architecture of a WDM-PON. As the downstream and upstream signals are transmitted over different wavelength bands in the carrier-distributed WDM-PON, RB from the upstream signal will not interfere with the downstream signal, and vice versa. Thus, the downstream channels are omitted in Fig. 1 for simplicity. The multi-wavelength optical carriers for upstream transmission are generated by continuous-wave (CW) lasers at the OLT as centralized light sources (CLS), and then multiplexed by an AWG. After the transmission in a feeder fiber with a length of L_1, the optical carriers are wavelength routed toward different ONUs, by another AWG at the remote node (RN). The length of the distribution fiber (between RN and ONU) is L_2. At ONU, the CW light is first amplified and then modulated by an optical phase modulator (PM), driven by differentially pre-coded upstream data, before being sent back to the OLT. Due to DI's periodic frequency response, all the upstream DPSK channels could be simultaneously demodulated by a common DI at the OLT [21]. Athermal DIs, with C+L band coverage by a single device, are commercially available. As both the CLS and the DI are located at CO, their wavelength alignment could be readily achieved by locking the CLS wavelength to the DI. Note that only the destructive port of the DI can be used for upstream DPSK demodulation and carrier RB suppression simultaneously [18], due to its notch filter-like frequency response. The demodulated DPSK signals are pre-amplified before direct detection. Proper dispersion compensation may be required depending on the reach of WDM-PON.

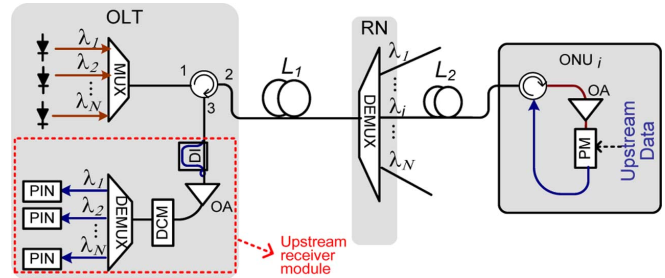

Fig. 1. Proposed loopback architecture using DPSK as the upstream modulation format to suppress Rayleigh noise. The downstream channels are omitted here for simplicity. OA: optical amplifier, PM: phase modulator, DI: delay-interferometer, DCM: dispersion compensation module, PIN: p-i-n receiver.

B. The Source of Rayleigh Noise

Rayleigh crosstalk is induced by the beating between the upstream signal and the in-band RB noise towards the OLT. Two types of RB exist: the carrier RB and the signal RB. The carrier RB arises from the CW carrier delivered to the ONU, whereas the signal RB is the back reflection of the upstream signal, which is further amplified and modulated at ONU before transmitting to the OLT, along with the upstream signal. By calculating the power ratio between two types of RB, we can find out their different contributions in the upstream Rayleigh noise.

We first calculate the power of carrier RB at port 2 of the OLT optical circulator. The signal RB is generated in both feeder and distribution fiber. The mean intensity of the carrier RB generated in the feeder fiber is given by

$$P_{\mathrm{CB\_1}} = \frac{P_C}{R_1} \tag{1}$$

where P_C is the power of optical carrier incident to the feeder fiber, and R_1 is the RB-induced return loss of the feeder fiber that is given by [22], [23],

$$R_1 = \frac{2}{S\left(1 - e^{-2\alpha_p L_1}\right)} \tag{2}$$

with S, α_p being the recapture factor, and fiber attenuation coefficient in units of km^{-1}, respectively. The values of S and α_p are set to be 0.0016 and 0.046, respectively, for the SMF used in the experiment. At port 2 of the OLT optical circulator, the mean intensity of the carrier RB generated in the distribution fiber is given by

$$P_{\text{CB\_2}} = \frac{P_C}{\alpha_1 \cdot \alpha_A} \cdot \frac{1}{R_2} \cdot \frac{1}{\alpha_A \cdot \alpha_1} = \frac{P_C}{(\alpha_1 \cdot \alpha_A)^2 \cdot R_2} \tag{3}$$

where α_1, α_A, are the insertion loss of the feeder fiber and the AWG at RN in linear scale, respectively, and R_2 is the RB-induced return loss of the distribution fiber. The insertion loss of AWGs used in this paper is 4 dB, thus the value of α_A is 2.5. Note that linear scale units are used for the parameters in all the equations of this paper, unless specified otherwise. α_1 and R_2 are given by

$$\alpha_1 = e^{\alpha_p L_1} \tag{4}$$

$$R_2 = \frac{2}{S\left(1 - e^{-2\alpha_p L_2}\right)} \tag{5}$$

Similarly, we can calculate the power of signal RB at port 2 of the OLT optical circulator. The mean intensity of the signal RB generated in the feeder fiber is given by

$$\begin{aligned} P_{\text{SB\_1}} = {} & \left(\frac{P_C}{\alpha_1 \cdot \alpha_A \cdot \alpha_2} \cdot G_{\text{ONU}} \cdot \frac{1}{\alpha_2 \cdot \alpha_A}\right) \cdot \frac{1}{R_1} \cdot \frac{1}{\alpha_A \cdot \alpha_2} \\ & \cdot G_{\text{ONU}} \cdot \frac{1}{\alpha_2 \cdot \alpha_A \cdot \alpha_1} = \frac{P_C \cdot G_{\text{ONU}}^2}{R_1 \cdot \alpha_1^2 \cdot (\alpha_A \cdot \alpha_2)^4} \end{aligned} \tag{6}$$

with α_2 and G_{ONU} being the insertion loss of the distribution fiber and the ONU gain, respectively. The ONU gain is defined as the power ratio between the output and the input signals at ONU. α_2 is further given by

$$\alpha_2 = e^{\alpha_p L_2} \tag{7}$$

The mean intensity of the signal RB generated in the distribution fiber is given by

$$\begin{aligned} P_{\text{SB\_2}} &= \left(\frac{P_C}{\alpha_1 \cdot \alpha_A \cdot \alpha_2} \cdot G_{\text{ONU}}\right) \cdot \frac{1}{R_2} \cdot G_{\text{ONU}} \cdot \frac{1}{\alpha_2 \cdot \alpha_A \cdot \alpha_1} \\ &= \frac{P_C \cdot G_{\text{ONU}}^2}{R_2 \cdot (\alpha_1 \cdot \alpha_A \cdot \alpha_2)^2} \end{aligned} \tag{8}$$

The power ratio between $P_{\text{CB\_1}}$ and $P_{\text{CB\_2}}$ can be derived via dividing (1) by (3) and similarly $P_{\text{SB\_1}}/P_{\text{SB\_2}}$ can be derived via dividing (6) by (8), as shown in Fig. 2. Note that Fig. 2 is independent of ONU gain and all types of RB powers are calculated at port 2 of the OLT optical circulator. An interesting point is that while the carrier RB generated in the feeder fiber is dominant, signal RB generated in a short distribution fiber may be comparable with or even larger than that generated in a long feeder fiber. As shown in Fig. 2, the signal RB generated in a 2-km distribution fiber can be even larger than that generated in an 80-km feeder fiber.

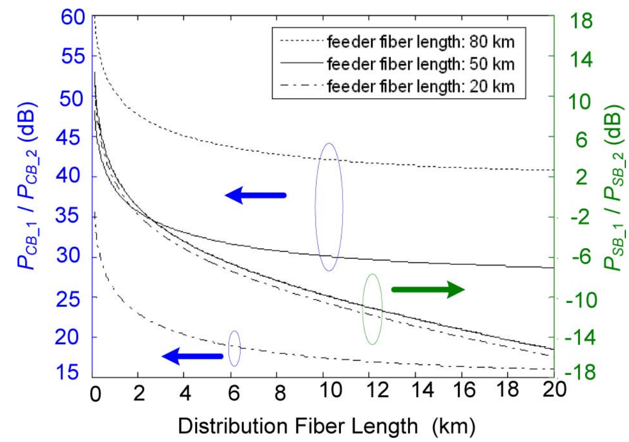

Fig. 2. $P_{\text{CB\_1}}/P_{\text{CB\_2}}$ and $P_{\text{SB\_1}}/P_{\text{SB\_2}}$ for different feeder and distribution fiber lengths. Two $P_{\text{SB\_1}}/P_{\text{SB\_2}}$ curves, for 50-km and 80-km feeder fibers respectively, are overlapped.

From (1)–(8), the power ratio between the two types of RB at port 2 of the OLT optical circulator can be derived as

$$\begin{aligned} \frac{P_{\text{CB}}}{P_{\text{SB}}} &= \frac{P_{\text{CB\_1}} + P_{\text{CB\_2}}}{P_{\text{SB\_1}} + P_{\text{SB\_2}}} \\ &= \frac{\left[(\alpha_1 \cdot \alpha_A)^2 \cdot R_2 + R_1\right] \cdot \alpha_2^4 \cdot \alpha_A^2}{G_{\text{ONU}}^2 \cdot \left[(\alpha_2 \cdot \alpha_A)^2 \cdot R_1 + R_2\right]} \end{aligned} \tag{9}$$

The required G_{ONU} can be further derived, from the power budget equation, as

$$G_{\text{ONU}} = \frac{M \cdot P_{\text{rec}} \cdot (\alpha_1 \cdot \alpha_A \cdot \alpha_2)^2 \cdot \alpha_{\text{Cir}}}{P_C} \tag{10}$$

with M, P_{rec} and α_{Cir} being the system margin, the minimum received upstream power needed to achieve $\text{BER} = 10^{-9}$, and the insertion loss from port 2 to 3 of the circulator at OLT, respectively. Note that the received upstream power is measured at the input port of DI. A link margin of 6–8 dB is generally used for future-proof fiber systems [24]. In this part, we use an 8-dB margin in the analysis. For 10-Gb/s DPSK signal, the back-to-back receiver sensitivity $(\text{BER} = 10^{-9})$ is measured to be around −32 dBm. If all the transmission impairments can be eliminated at the upstream receiver module, we can substitute this sensitivity value as P_{rec} into (10) to calculate the required ONU gain for different system reaches. The input power to the feeder fiber is assumed to be $P_C = 3$ dBm. Then, by substituting the calculated ONU gain to (9), we can further calculate the power ratio between two types of RB for different system reaches, with considering different length ratios between the feeder and distribution fibers. As shown in Fig. 3, we can observe that the carrier RB is more than 20-dB larger than the signal RB, implying that carrier RB is the dominant noise entering the upstream receiver module. In practical implementation, the transmission impairments may not be fully eliminated at the upstream receiver module (i.e., there may be residual

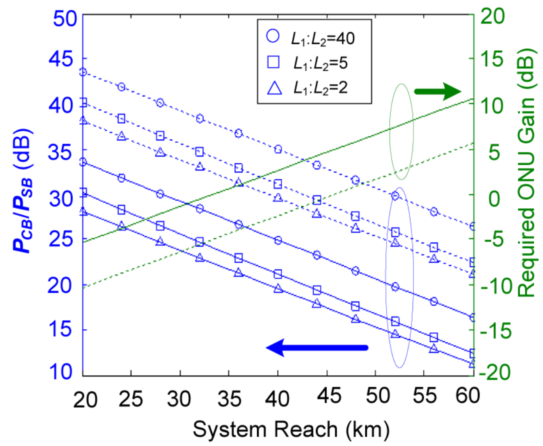

Fig. 3. Required ONU gain, and $P_{\rm CB}/P_{\rm SB}$ for different system reaches. The minimum received upstream power needed to achieve $\text{BER} = 10^{-9}$ is set to be -32 dBm for the dashed line, and -27 dBm for the solid line, respectively.

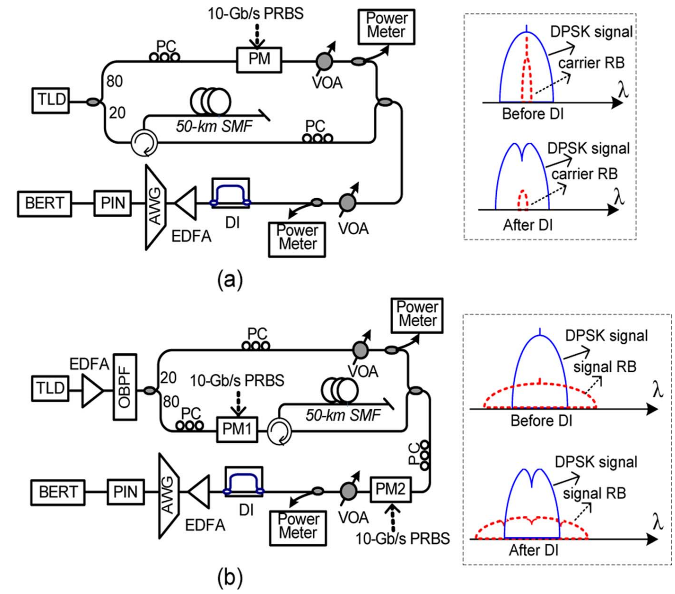

Fig. 4. Experimental setup to investigate the effectiveness of the proposed scheme on the suppression of (a) carrier RB, and (b) signal RB. Insets: sketches of the spectrum of the DPSK signal, carrier RB and signal RB, before and after the DI.

Rayleigh noise or dispersion.), thus we further calculate the required ONU gain and the power ratio between two types of RB, with additional power penalty of 5 dB (i.e., $P_{\rm rec} = -27$ dBm) after transmission. The calculated results are also shown in Fig. 3. Obviously, the carrier RB is still the dominant noise entering the upstream receiver module in this scenario, even after 60-km transmission. Based on the aforementioned analysis, we conclude that the suppression of carrier RB should be the main consideration in the design of RB-reduced upstream receiver.

III. Effectiveness of the Proposed Scheme on RB Reduction and Transmission Demonstration

A. *Effective Suppression for Carrier RB Only*

We investigated the upstream power penalty as a function of signal-to-crosstalk ratio (SCR) based on the experimental setup in Fig. 4, which is similar to that employed in [14]. We first used carrier RB as the crosstalk signal, as in Fig. 4(a). CW light at 1553.5 nm with a line width of 100 kHz was generated from a tunable laser diode (TLD) and was split into two paths by an 80/20 coupler. In the upper path, a PM was driven by a 10-Gb/s $2^{31} - 1$ pseudorandom binary sequence (PRBS) to generate the DPSK signal. Following the PM, a variable optical attenuator (VOA) was used to adjust the signal power to obtain different SCR values. In the lower path, the crosstalk signal was the RB light from a 50-km SMF, with a fixed power of -30 dBm measured after a polarization controller (PC). The PC was used to maximize the beating noise. The DPSK signal and the crosstalk signal were then combined by a 3-dB coupler and fed into the proposed upstream receiver module, which consisted of a 94-ps DI with a measured ER of 22 dB, an EDFA, a 100-GHz AWG ($\text{3-dB bandwidth} = 0.35$ nm, $\text{insertion loss} = 4$ dB), and a p-i-n receiver. The carrier RB with a very narrow spectrum can be effectively rejected by the DI's destructive port that is also used as a DPSK demodulator, as illustrated in the inset of Fig. 4(a). The measured crosstalk tolerance of the DPSK signal is shown in Fig. 5. For comparison, the crosstalk tolerance of the conventional OOK signal was also measured. In this case, the PM was replaced by a Mach-Zehnder modulator (MZM) and the

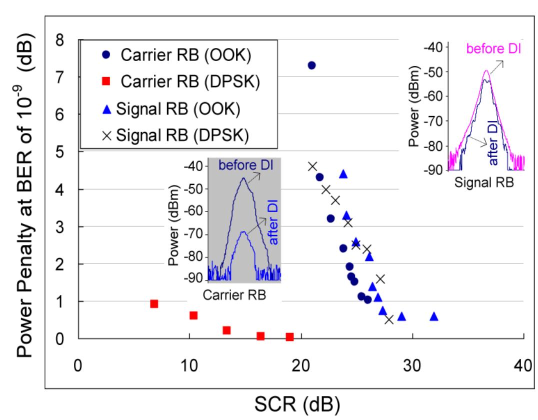

Fig. 5. Power penalty as a function of signal-to-crosstalk ratio (SCR). Insets: measured spectra ($\text{resolution bandwidth} = 0.06$ nm) of signal (DPSK) RB and carrier RB before and after DI.

DI was removed from the upstream receiver module. Compared with the conventional scheme using OOK format, the carrier-RB tolerance of the proposed scheme is substantially improved by 19 dB, as shown in Fig. 5.

Then signal RB was used as the crosstalk signal, as in Fig. 4(b). In the lower path PM1 was used to generate the signal RB, which was further combined with the optical carrier in the upper path. The combined light was then modulated by PM2, which was used to generate the upstream DPSK signal. In the lower path the power of signal RB was fixed at -32 dBm and different SCR values could be obtained by adjusting the VOA in the upper path. Again, for comparison, the signal-RB tolerance of the conventional OOK signal was also measured by replacing PM1 and PM2 with two MZMs and removing the DI from the upstream receiver module. The measurement results are also shown in Fig. 5. We can find that the signal-RB tolerance is not improved in the proposed scheme. The reason is that the signal RB has a wide spectrum after being modulated twice and thus cannot be effectively suppressed by DI's destructive port, as illustrated in the inset of Fig. 4(b). We also measured the spectra of the carrier RB and signal RB, before and after the DI. As observed from the measured spectra ($\text{resolution bandwidth} = 0.06$ nm) in the insets of Fig. 5, the carrier RB is substantially suppressed by DI's destructive port, whereas the signal-RB only experiences little suppression.

Although the proposed scheme can only suppress the carrier RB, it is sufficient to significantly improve the system's tolerance to Rayleigh noise, due to the aforementioned fact that the carrier RB is the dominant noise.

B. Transmission Demonstration

We then experimentally demonstrated the effectiveness of the proposed loopback scheme based on the architecture shown in Fig. 1. At the OLT, CW light at 1553.5 nm from a TLD with a power of 3-dBm was fed into a span of 50-km SMF through a circulator (from port 1 to port 2). An AWG (4-dB insertion loss) with a channel spacing of 0.8 nm and a 3-dB bandwidth of 0.6 nm was used at the RN. After transmission through another 10-km SMF (the distribution fiber), the CW light with a power of -13.5 dBm was fed into the ONU, which consisted of a circulator, an EDFA and a PM. The PM was driven by a 10-Gb/s $2^{31}-1$ PRBS to generate the upstream DPSK signal, which was looped back to the OLT through the ONU circulator. A commercially available single-arm $LiNbO_3$ PM was used in this proof-of-concept experiment, but some polarization-insensitive integrated PMs could be more desirable for practical applications [25], [26]. In addition, a semiconductor optical amplifier could also be used as a PM [27]. The upstream receiver module here was the same as in Fig. 4, except that a dispersion compensation module (DCM, -666 ps/nm @ 1545 nm) is added to compensate around 2/3 of the accumulated dispersion for the upstream signal. The accumulated dispersion was not fully compensated, as in practical implementation all the upstream channels cannot be simultaneously fully compensated by a common DCM due to the length variation of distribution fibers.

The BER measurement results are shown in Fig. 6. Note that the received optical power was measured before the input port of DI, and the ONU gain was fixed at 11 dB for all BER measurements. Compared with the back-to-back cases, around 4.5-dB power penalty ($\text{BER} = 10^{-9}$) is observed for the upstream DPSK signal after 60-km transmission, due to the residual dispersion and the residual Rayleigh noise. To further investigate the power penalty induced by the residual Rayleigh noise, the BER curve after 60-km transmission in dual fibers is also shown in Fig. 6. Comparing the single-fiber and dual-fiber curves, less than 2.4-dB Rayleigh noise-induced power penalty is observed, showing the effectiveness of the proposed scheme in Rayleigh noise reduction. For this transmission experiment, the calculated SCR levels are around 10.6 dB and 22.3 dB for the carrier RB and signal RB, respectively. According to Fig. 5, power penalties induced by carrier RB and signal RB should be $\sim$0.7 dB and ~ 4 dB, respectively, under these specific SCR levels. We notice that the measured 2.4-dB Rayleigh noise-induced power penalty is less than the predicted value by Fig. 5, due to the fact

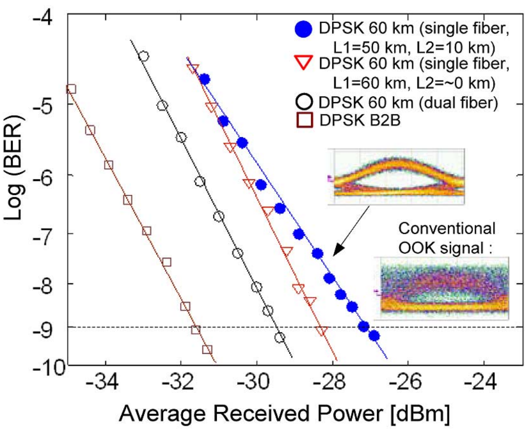

Fig. 6. BER measurement results. Insets: upstream eye diagrams in the proposed scheme and in the conventional scheme. Time scale: 20 ps/div.

that in the transmission experiment the polarization planes of the upstream signal and Rayleigh noise cannot be always coincided as in the back-to-back experiment to obtain the results in Fig. 5. Rayleigh noise-induced power penalty will be further decreased when the length of distribution fiber is reduced. As shown in Fig. 6, Rayleigh noise-induced power penalty is reduced to 1.2 dB, for the extreme case when the total transmission link consists of only feeder fiber ($L_1 = 60$ km and $L_2 =\sim 0$ km). In this case, the SCR level of the carrier RB is still around 10.6 dB, whereas the SCR level of the signal RB is increased from 22.3 dB to 28.5 dB.

We also compared the proposed scheme with that using conventional OOK modulation in upstream. We replaced the PM in Fig. 1 with a MZM, removed the DI from OLT, and maintained the same ONU gain. While an error floor above 10^{-6} was observed for the upstream OOK signal in the 20-km demonstration in [18], in this 60-km experiment ($\text{L1} = 50$ km and $\text{L2} = 10$ km) the upstream OOK BER even could not be measured due to significant degradation by Rayleigh noise. In contrast to the wide-open eye diagram of the demodulated upstream DPSK signal, a much degraded eye diagram of the upstream OOK signal is also shown in the insets of Fig. 6.

C. The Effect of DI's ER and Optical Carrier's Line Width

We have demonstrated that DI's destructive port can effectively suppress the carrier RB, due to its notch filter-like frequency response. Here we will further study the dependence of carrier RB suppression on DI's ER and optical carrier's line width.

From self-homodyne theory [28], the output power from one output port of DI can be expressed as:

$$P_o = P_1 + P_2 + 2\sqrt{P_1 P_2}\cos(\Delta T \cdot \omega + \varphi_0) \tag{11}$$

where P_1 and P_2 are the powers delivered to an output port from two arms of the DI, respectively, ΔT is the relative delay between two arms of the DI, ω is the angular frequency of optical carrier, and φ_0 is the phase-setting constant of the DI. The relation between P_1, P_2 and DI's input power P_i is determined by the coupling ratios of the two couplers in the DI and the insertion loss of the two arms. From (11), we can rewrite the transfer function of DI as:

$$f_{\mathrm{DI}}(\omega) = \frac{P_o}{P_i} = a + b\cos(\Delta T \cdot \omega + \varphi_0) \tag{12}$$

with a and b being two undetermined coefficients at this moment. The constructive and destructive ports have different φ_0. For the optical carrier with a certain frequency of ω_0, the transfer function of the destructive port of DI can be expressed as:

$$f_{\mathrm{DP}}(\omega) = a + b\cos(\Delta T \cdot \omega + \pi - \Delta T \cdot \omega_0) \tag{13}$$

Let $\mathrm{ER_{DI}}$ denote the extinction ratio of the DI, coefficients a and b should fulfill the following conditions (14) and (15):

$$0 < a + b \leq 1, \tag{14}$$

$$\frac{a+b}{a-b} = \mathrm{ER_{DI}} \tag{15}$$

The power spectral density (PSD) of carrier RB can be expressed as [22],

$$S_b(\omega) \approx \langle I_b \rangle^2 \left(2\pi\delta(\omega - \omega_0) + \frac{2\Delta\omega}{\Delta\omega^2 + (\omega - \omega_0)^2} \right) \tag{16}$$

where $\langle I_b \rangle^2$ is the mean backscattered intensity determined by the property of the fiber for a given input signal to the fiber, $\Delta\omega$ denotes the full width at half-maximum of the Lorentzian shaped laser spectrum.

The average reflection power P_r is:

$$P_r = \int_{-\infty}^{+\infty} S_b(\omega) d\omega \tag{17}$$

After passing through a DI, the average reflection power P_r' at DI's destructive port is:

$$P_r' = \int_{-\infty}^{+\infty} f_{\mathrm{DP}}(\omega) S_b(\omega) d\omega \tag{18}$$

From (13)–(18), we can get the carrier-RB suppression ratio by DI's destructive port as:

$$\begin{aligned} S_{\mathrm{DI}}(dB) &= 10\log\left(\frac{P_r}{P_r'}\right) \\ &= 10\log\left[\frac{4}{(a+b)\cdot\left(\frac{\mathrm{ER_{DI}}+3}{\mathrm{ER_{DI}}} - \frac{\mathrm{ER_{DI}}-1}{\mathrm{ER_{DI}}} e^{-\Delta\omega\cdot\Delta T}\right)}\right] \end{aligned} \tag{19}$$

Based on (19) we can obtain the dependence of carrier RB suppression on DI's extinction ratio $\mathrm{ER_{DI}}$ and the laser's linewidth $\Delta\omega$, as depicted in Fig. 7. For an ideal DI, $a + b = 1$. In practice, $(a + b)$ is smaller than 1 due to various reasons, such as unequal coupling ratios of the two couplers in the DI and polarization misalignment. Nevertheless, $(a + b)$ should be close to 1 for common cases. Note that Fig. 7 is derived with the assumption of $a + b = 1$. Interestingly, as shown in

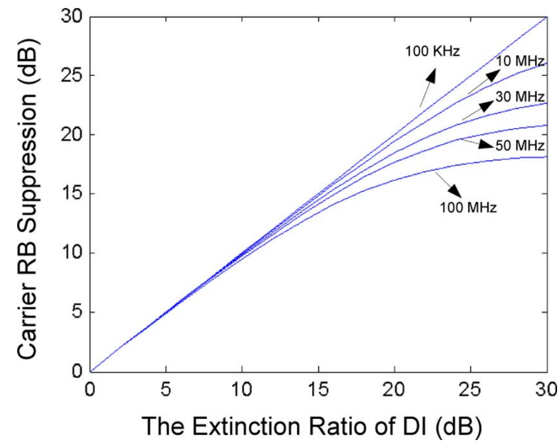

Fig. 7. Dependence of carrier RB suppression on DI's extinction ratio and laser's linewidth.

Fig. 7, carrier RB suppression is predominantly determined by DI's ER when DI's ER is low, whereas it is determined by both laser's linewidth and DI's ER when DI's ER is high.

IV. Relation Between System Margin and ONU Gain

According to the experimental results in Fig. 6, the minimum received upstream power needed to achieve $\mathrm{BER} = 10^{-9}$ is -26.7 dBm when $L_1 = 50$ km, $L_2 = 10$ km, and $G_{\mathrm{ONU}} = 11$ dB. Meanwhile, the measured average received power by the upstream receiver module is -18.7 dBm, implying 8-dB system margin. In practice, the required system margin may vary with different service quality requirements and different external transmission environments. On the other hand, for a given input power to the feeder fiber, system margin is determined by the minimum received upstream power needed to achieve $\mathrm{BER} = 10^{-9}$ and ONU gain. Next we will investigate the relation between the minimum received upstream power needed to achieve $\mathrm{BER} = 10^{-9}$ and ONU gain, from which the relation between system margin and ONU gain can also be derived through straightforward calculation.

At the upstream receiver in OLT, the signal-RB beating noise and signal-amplified spontaneous emission (ASE) beating noise are dominant. The optical signal-to-noise ratio (OSNR) before the p-i-n receiver is given by

$$\begin{aligned} \mathrm{OSNR} &= \frac{P_S' \cdot G_{\mathrm{OLT}}}{(P_{\mathrm{CB}}' + P_{\mathrm{SB}}') \cdot G_{\mathrm{OLT}} + P_{\mathrm{ASE}}} \\ &= \frac{1}{\frac{P_{\mathrm{CB}}'}{P_S'} + \frac{P_{\mathrm{SB}}'}{P_S'} + \frac{1}{P_S'} \cdot \frac{P_{\mathrm{ASE}}}{G_{\mathrm{OLT}}}} \end{aligned} \tag{20}$$

where P_S', P_{CB}' and P_{SB}' are the optical power of the upstream signal, the carrier RB and the signal RB, respectively, before the optical preamplifier at OLT. G_{OLT} and P_{ASE} are the gain of the preamplifier, and the power of ASE noise within the passband of an AWG channel, respectively. The ASE noise generated during ONU amplification is neglected, as after transmitting to the upstream receiver it is significantly smaller than both Rayleigh noise and the ASE noise that is generated at OLT.

Equation (20) can be rewritten as

$$P'_S = \frac{P_{\mathrm{ASE}}/G_{\mathrm{OLT}}}{1/\mathrm{OSNR} - P'_{\mathrm{SB}}/P'_S - P'_{\mathrm{CB}}/P'_S} \tag{21}$$

where

$$\frac{P_{\mathrm{ASE}}}{G_{\mathrm{OLT}}} \approx h\nu n_{\mathrm{sp}} \cdot \Delta\nu_{\mathrm{opt}}, \quad (G_{\mathrm{OLT}} \gg 1) \tag{22}$$

with $h, \nu, n_{\mathrm{sp}}, \Delta\nu_{\mathrm{opt}}$ being the Planck constant, the optical frequency, the spontaneous-emission factor ($n_{\mathrm{sp}} = 2$ in this paper) and the channel bandwidth of the OLT AWG, respectively [24].

Assume the BER of the upstream signal is 10^{-9} when the optical signal-to-noise ratio equals to a specific value of OSNR_0. Then based on (21), the minimum received upstream power needed to achieve $\mathrm{BER} = 10^{-9}$ can be expressed as,

$$P_{\mathrm{rec}} = \frac{P_{\mathrm{ASE}}/G_{\mathrm{OLT}}}{1/\mathrm{OSNR}_0 - P'_{\mathrm{SB}}/P'_S - P'_{\mathrm{CB}}/P'_S} \cdot \alpha_{\mathrm{DI}} \tag{23}$$

$P'_{\mathrm{SB}}, P'_{\mathrm{CB}}$, and P'_S are determined by the following two equations,

$$P'_{\mathrm{SB}} = (P_{\mathrm{SB\_1}} + P_{\mathrm{SB\_2}})/\alpha_{\mathrm{Cir}}/\alpha_{\mathrm{DI}} \tag{24}$$

$$P'_{\mathrm{CB}} = (P_{\mathrm{CB\_1}} + P_{\mathrm{CB\_2}})/\alpha_{\mathrm{Cir}}/S_{\mathrm{DI}} \tag{25}$$

$$P'_S = \frac{P_C \cdot G_{\mathrm{ONU}}}{(\alpha_1 \cdot \alpha_A \cdot \alpha_2)^2 \cdot \alpha_{\mathrm{Cir}} \cdot \alpha_{\mathrm{DI}}} \tag{26}$$

Since both the upstream signal and the signal RB experience very similar loss when passing through the DI, we use a common symbol α_{DI} to denote DI's insertion loss for the signal RB in (24) as well as for the upstream signal in (26). α_{DI} was measured to be $\sim$4 dB. S_{DI} is the carrier-RB suppression ratio by DI's destructive port in linear scale and can be derived from (19).

Based on the experimental results and (1)–(8), (19) and (24)–(26), we can derive the value of OSNR_0 and can rewrite (23) as,

$$P_{\mathrm{rec}} = \frac{k_3}{k_0 - k_1 \cdot G_{\mathrm{ONU}} - \frac{k_2}{G_{\mathrm{ONU}}}} \tag{27}$$

with k_0, k_1, k_2 and k_3 being

$$k_0 = 1/\mathrm{OSNR}_0$$
$$k_1 = \frac{1}{(\alpha_2 \cdot \alpha_A)^2 \cdot R_1} + \frac{1}{R_2}$$
$$k_2 = \frac{\alpha_{\mathrm{DI}} \cdot \alpha_2^2 \cdot \left[R_1 + (\alpha_1 \cdot \alpha_A)^2 \cdot R_2\right]}{S_{\mathrm{DI}} \cdot R_1 \cdot R_2}$$
$$k_3 = h\nu n_{\mathrm{sp}} \cdot \Delta\nu_{\mathrm{opt}} \cdot \alpha_{\mathrm{DI}}$$

Then based on (27) we can plot the relation between the minimum received upstream power needed to achieve $\mathrm{BER} = 10^{-9}$ and ONU gain as in Fig. 8. Note that the parameters used in the theoretical calculations are in correspondence with the experimental setup. In Fig. 8, the large difference between the case for $60\ \mathrm{km} + 0$ km and the case for $50\ \mathrm{km} + 10$ km is due to the fact that the signal RB, which cannot be suppressed by DI's destructive port, is significantly increased when the distribution fiber is increased to 10 km, as illustrated in Fig. 2. To confirm

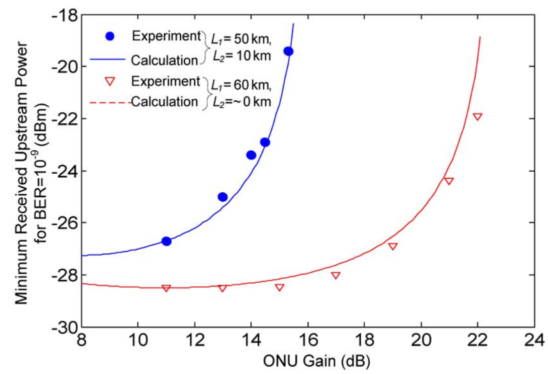

Fig. 8. The relation between the minimum received upstream power needed to achieve $\mathrm{BER} = 10^{-9}$ and ONU gain.

the correctness of theoretical analysis described above, the minimum received upstream powers (to achieve $\mathrm{BER} = 10^{-9}$) corresponding to different ONU gains were measured in experiment and are also shown in Fig. 8. Good agreement between the theory and experiment is observed. The theoretical model predicts well the system performance and thus can be used as a guideline in system design. As an example, based on the aforementioned theoretical model the optimal ONU gain can be derived to maximize the system margin.

Equation (10) can be rewritten as

$$M = \frac{P_C}{(\alpha_1 \cdot \alpha_A \cdot \alpha_2)^2 \cdot \alpha_{\mathrm{Cir}}} \cdot \frac{G_{\mathrm{ONU}}}{P_{\mathrm{rec}}} \tag{28}$$

Substituting (27) into (28), we can derive,

$$M = \frac{P_C}{(\alpha_1 \cdot \alpha_A \cdot \alpha_2)^2 \cdot \alpha_{\mathrm{Cir}}} \cdot \frac{-k_1 \cdot G_{\mathrm{ONU}}^2 + k_0 \cdot G_{\mathrm{ONU}} - k_2}{k_3} \tag{29}$$

From (29), we can further derive that the maximum system margin can be achieved as

$$M_{\mathrm{Max}} = \frac{P_C}{(\alpha_1 \cdot \alpha_A \cdot \alpha_2)^2 \cdot \alpha_{\mathrm{Cir}}} \cdot \frac{k_0^2 - 4k_1 \cdot k_2}{4k_1 \cdot k_3} \tag{30}$$

when the ONU gain is optimized as

$$G_{\mathrm{ONU\_Opt}} = k_0/2k_1 \tag{31}$$

Then based on (30) and (31) we can calculate the maximum system margin and the required optimal ONU gain for different system reaches with different feeder-distribution length ratios, as in Fig. 9. Interestingly, with certain length ratio the optimal gain is nearly constant for reach ranging from 55 km to 75 km. Note that for the scheme employing conventional OOK in upstream, the variation of optimal ONU gain is 8 dB (20 km $\times$ 0.2 dB/km $\times$ 2) for a 20-km change in system reach [19]. Thus, an attractive feature of the proposed scheme is that all ONU's with similar length ratios can be set to a fixed gain even for a large change in system reach, avoiding the incurred operation complexity of setting different gains for ONUs with different reaches.

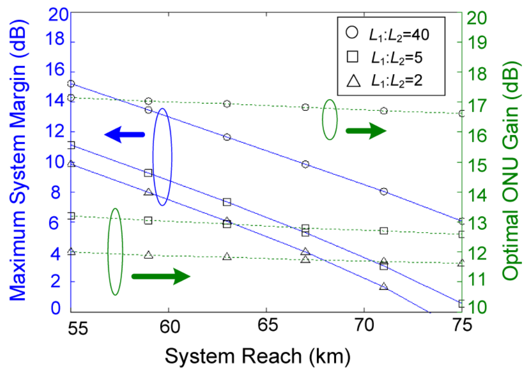

Fig. 9. The maximum system margin and the required optimal ONU gain for different system reaches.

V. Conclusion

In this paper, we provide an insight into different design issues for Rayleigh noise mitigation in carrier-distributed WDM-PON. For the first time, we clarify that two types of RB are not comparable in impairing the upstream signal, with carrier RB being the dominant noise entering the Rayleigh noise-reduced upstream receiver module, within a reach up to 60 km. Then we propose a simple scheme, via in-band optical filtering, to effectively suppress carrier RB in the carrier-distributed WDM-PON, with a demonstrated 19-dB improvement in the tolerance to carrier RB. We also theoretically study the dependence of carrier RB suppression on DI's ER and optical carrier's line width. Error-free transmission of 10-Gb/s upstream signal over 60-km SMF is achieved with less than 2.5-dB power penalty induced by residual Rayleigh noise. The relation between system margin and ONU gain is also comprehensively studied. The theoretical model built in this paper predicts well the system performance and is expected to serve as a design tool for optimizing the overall performance of a WDM-PON.

References

[1] G. K. Chang, A. Chowdhury, Z. S. Jia, H. C. Chien, M. F. Huang, J. J. Yu, and G. Ellinas, "Key technologies of WDM-PON for future converged optical broadband access networks [invited]," *J. Opt. Commun. Netw.*, vol. 1, pp. C35–C50, 2009.

[2] N. J. Frigo, P. P. Iannone, P. D. Magill, T. E. Darcie, M. M. Downs, B. N. Desai, U. Koren, T. L. Koch, C. Dragone, H. M. Presby, and G. E. Bodeep, "A wavelength-division multiplexed passive optical network with cost-shared components," *IEEE Photon. Technol. Lett.*, vol. 6, no. 11, pp. 1365–1367, Nov. 1994.

[3] M. Feuer, M. Thomas, and L. Lunardi, "Backreflection and loss in single-fiber loopback networks," *IEEE Photon. Technol. Lett.*, vol. 12, no. 8, pp. 1106–1108, Aug. 2000.

[4] T. H. Wood, R. A. Linke, B. L. Kasper, and E. C. Carr, "Observation of coherent Rayleigh noise in single-source bidirectional optical fiber systems," *J. Lightw. Technol.*, vol. 6, no. 2, pp. 346–352, Feb. 1988.

[5] P. T. Legg, M. Tur, and I. Andonovic, "Solution paths to limit interferometric noise induced performance degradation in ASK/direct detection lightwave networks," *J. Lightw. Technol.*, vol. 14, no. 9, pp. 1943–1953, Sept. 1996.

[6] P. J. Urban, H. De Waardt, E. Ciaramella, and A. M. J. Koonen, "Reduction of the influence of optical interferometric crosstalk noise in a WDM-PON system with a reflective semiconductor optical amplifier: An overview," in *Proc. ICTON*, 2010, paper Tu.B1.4.

[7] I. T. Monroy, E. Tangdiongga, R. Jonker, and H. de Waardt, "Interferometric crosstalk reduction by phase scrambling," *J. Lightw. Technol.*, vol. 18, no. 5, pp. 637–646, May 2000.

[8] M. Feuer, M. Thomas, and L. Lunardi, "Backreflection and loss in single fiber loopback networks," *IEEE Photon. Technol. Lett.*, vol. 12, no. 8, pp. 1106–1108, Aug. 2000.

[9] A. Chiuchiarelli, M. Presi, R. Proietti, G. Contestabile, P. Choudhury, L. Giorgi, and E. Ciaramella, "Enhancing resilience to Rayleigh crosstalk by means of line coding and electrical filtering," *IEEE Photon. Technol. Lett.*, vol. 22, no. 2, pp. 85–87, Jan. 15, 2010.

[10] D. Jorgesen, C. F. Marki, and S. Esener, "Improved high pass filtering for passive optical networks," *IEEE Photon. Technol. Lett.*, vol. 22, no. 8, pp. 1144–1146, Aug. 2010.

[11] J. Prat, "Rayleigh back-scattering reduction by means of quantized feedback equalization in WDM-PONs," presented at the ECOC, 2010, paper Th.10.B.3.

[12] P. J. Urban, A. M. J. Koonen, G. D. Khoe, and H. de Waardt, "Interferometric crosstalk reduction in an RSOA-based WDM passive optical network," *J. Lightw. Technol.*, vol. 27, no. 11, pp. 4943–4953, Nov. 2009.

[13] T. Yoshida, S. Kimura, H. Kimura, K. Kumozaki, and T. Imai, "A new single-fiber 10-Gb/s optical loopback method using phase modulation for WDM optical access networks," *J. Lightw Technol.*, vol. 24, no. 2, pp. 786–796, Feb. 2006.

[14] C. W. Chow, G. Talli, and P. D. Townsend, "Rayleigh noise reduction in 10-Gb/s DWDM-PONs by wavelength detuning and phase-modulation-induced spectral broadening," *IEEE Photon. Technol. Lett.*, vol. 19, no. 6, pp. 423–425, Mar. 2007.

[15] A. Chowdhury, H.-C. Chien, M.-F. Huang, J. Yu, and G.-K. Chang, "Rayleigh backscattering noise-eliminated 115-km long-reach bidirectional centralized WDM-PON with 10-Gb/s DPSK downstream and remodulated 2.5-Gb/s OCS-SCM upstream signal," *IEEE Photon. Technol. Lett.*, vol. 20, no. 24, pp. 2081–2083, Dec. 2008.

[16] C. W. Chow, G. Talli, A. D. Ellis, and P. D. Townsend, "Rayleigh noise mitigation in DWDM LR-PONs using carrier suppressed subcarrier-amplitude modulated phase shift keying," *Opt. Expr.*, vol. 16, no. 3, pp. 1860–1866, Feb. 2008.

[17] J. Xu and L. K. Chen, "Optical phase remodulation for 10-Gb/s WDM-PON with enhanced tolerance to Rayleigh noise," presented at the OFC/NFOEC, 2010, Paper OThG3.

[18] J. Xu, L. K. Chen, and C. K. Chan, "Phase-modulation-based loopback scheme for Rayleigh noise suppression in 10-Gb/s carrierdistributed WDM-PONs," *IEEE Photon. Technol. Lett.*, vol. 22, no. 18, pp. 1343–1345, Sep. 2010.

[19] M. Fujiwara, J. Kani, H. Suzuki, and K. Iwatsuki, "Impact of backreflection on upstream transmission in WDM single-fiber loopback access networks," *J. Lightw. Technol.*, vol. 24, no. 2, pp. 740–746, Feb. 2006.

[20] K. Y. Cho, Y. J. Lee, H. Y. Choi, A. Murakami, A. Agata, Y. Takushima, and Y. C. Chung, "Effects of reflection in RSOA-based WDM PON utilizing remodulation technique," *J. Lightw. Technol.*, vol. 27, no. 10, May 2009.

[21] X. Liu, A. H. Gnauck, X. Wei, J. Y. C. Hsieh, and V. Chien, "A thermal optical demodulator for OC-768 DPSK and RZ-DPSK signals," *IEEE Photon. Technol. Lett.*, vol. 17, no. 12, pp. 2610–2612, Dec. 2005.

[22] P. Gysel and R. K. Staubli, "Statistical properties of Rayleigh backscattering in single-mode fibers," *J. Lightwave Technol.*, vol. 8, no. 4, pp. 561–567, Apr. 1990.

[23] S. K. Liaw, S. L. Tzeng, and Y. J. Hung, "Rayleigh backscattering induced power penalty on bidirectional wavelength-reuse fiber systems," *Opt. Commun.*, vol. 188, no. 1–4, pp. 63–67, Feb. 2001.

[24] G. Keiser, *Optical Fiber Communications*, 3rd ed. New York: McGraw-Hill, 2000.

[25] F. Y. Gardes, K. L. Tsakmakidis, D. Thomson, G. T. Reed, G. Z. Mashanovich, and O. Hess, "Micrometer size polarization independent depletion-type photonic modulator in silicon on insulator," *Opt. Expr.*, vol. 15, no. 9, pp. 5879–5884, Apr. 2007.

[26] J. Zhang, T. Y. Liow, G. Q. Lo, and D. L. Kwong, "10 Gbps monolithic silicon FTTH transceiver without laser diode for a new PON configuration," *Opt. Expr.*, vol. 18, no. 5, pp. 5135–5141, 2010.

[27] S. P. Jung, Y. Takushima, and Y. C. Chung, "Transmission of 1.25-Gb/s PSK signal generated by using RSOA in 110-km coherent WDM PON," *Opt. Expr.*, vol. 18, pp. 14871–14877, 2010.

[28] D. Derickson, *Fiber Optic Test and Measurement*. Englewood Cliffs, NJ: Prentice-Hall, 1998.

Author biographies not included at author request due to space constraints.